Heliyon 10 (2024) e29484

Contents lists available at ScienceDirect

Heliyon

journal homepage: www.cell.com/heliyon

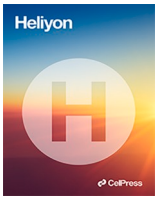

Research article

Neuroprotective effects of takinib on an experimental traumatic brain injury rat model via inhibition of transforming growth factor beta-activated kinase 1

Shuangying Hao [a,1], Shuai Yuan [a,1], Zhiqiang Liu [a], Baohua Hou [a], Sijie Feng [a,**], Dingding Zhang [b,*]

[a] School of Medicine, Henan Polytechnic University, Jiaozuo, Henan, PR China
[b] Department of Neurosurgery, Nanjing Drum Tower Hospital, The Affiliated Hospital of Nanjing University Medical School, Nanjing, Jiangsu, PR China

ARTICLE INFO

Keywords:
TBI
TAK1
Takinib
Inflammation
Apoptosis
Neuroprotection

ABSTRACT

Transforming growth factor β-activated kinase 1 (TAK1) plays a significant role in controlling several signaling pathways involved with regulating inflammation and apoptosis. As such, it represents an important potential target for developing treatments for traumatic brain injury (TBI). Takinib, a small molecule and selective TAK1 inhibitor, has potent anti-inflammatory activity and has shown promising activity in preclinical studies using rat models to evaluate the potential neuroprotective impact on TBI. The current study used a modified Feeney's weight-drop model to cause TBI in mature Sprague-Dawley male rats. At 30 min post-induction of TBI in the rats, they received an intracerebroventricular (ICV) injection of Takinib followed by assessment of their histopathology and behavior. The results of this study demonstrated how Takinib suppressed TBI progression in the rats by decreasing TAK1, *p*-TAK1, and nuclear p65 levels while upregulating IκB-α expression. Takinib was also shown to significantly inhibit the production of two pro-inflammatory factors, namely tumor necrosis factor-α and interleukin-1β. Furthermore, Takinib greatly upregulated the expression of tight junction proteins zonula occludens-1 and claudin-5, reducing cerebral edema. Additionally, Takinib effectively suppressed apoptosis via down-regulation of cleaved caspase 3 and Bax and reduction of TUNEL-positive stained cell count. As a result, an enhancement of neuronal function and survival was observed post-TBI. These findings highlight the medicinal value of Takinib in the management of TBI and offer an experimental justification for further investigation of TAK1 as a potential pharmacological target.

Abbreviations: TBI, traumatic brain injury; TAK1, Transforming growth factor β-activated kinase 1; SBI, secondary brain injury; NF-κB, nuclear factor kappa-B; BBB, blood-brain barrier; ELISA, enzyme-linked immunosorbent assay; NSS, neurological severity score; ZO-1, zonula occludens-1; TUNEL, the terminal deoxynucleotidyl transferase dUTP nick end-labeling; ICV, intracerebroventricular.

* Corresponding author.
** Corresponding author. School of Medicine, Henan Polytechnic University, Shiji Road 2001Jiaozuo, Henan, PR China.
E-mail addresses: fsj1992@hpu.edu.cn (S. Feng), zhangdingding2373@163.com, zhangding9856@126.com (D. Zhang).
[1] These authors have contributed equally to this work.

https://doi.org/10.1016/j.heliyon.2024.e29484
Received 3 November 2023; Received in revised form 7 April 2024; Accepted 8 April 2024
Available online 10 April 2024

1. Introduction

Traumatic brain injury (TBI) is a complicated, multi-faceted pathophysiological condition with significant morbidity and mortality rates, particularly among younger people. Important risks factors include warfare, automotive accidents, and contact sports [1]. Despite extensive research, no effective pharmacological therapies currently exist that significantly lower morbidity and death or improve overall outcomes in the clinical settings [2], requiring the development of new therapeutic strategies.

TBI occurs in two stages: primary brain injury and secondary brain injury (SBI). It has been previously observed that SBI can lead to continual neuronal degeneration that leads to brain damage over minutes to months. This is attributed to a complex of biochemical and molecular mechanisms, including excessive glutamate release, production of free oxygen radicals, lipid peroxidation, and endogenous neuroinflammation [3,4]. Although patient outcomes are primarily determined by the primary brain trauma, the subsequent SBI resulting from these biochemical and molecular mechanisms allows for possible clinical intervention [5].

Transforming growth factor beta-activated kinase 1 (TAK1), belonging to the mitogen-activated protein kinase kinase kinase (MAPKKK) family, is vital in tumor necrosis factor (TNF), interleukin 1 (IL-1), and Toll-like receptor (TLR) signaling pathways [6–8]. Previous studies have observed that TAK1 is activated after TBI occurs, and inhibition of its activity decreases the biochemical and molecular processes associated with TBI, including inflammation and apoptosis [9,10]. These findings suggest a potential avenue for manipulating this pathway in clinical practice.

Takinib (*N*-(1-propyl-1,3-dihydro-2H-benzo [*d*]imidazole-2-ylidene)isophthalamide) is a small molecule that selectively inhibits autophosphorylated TAK1. It decreases TAK1 activation by noncompetitively binding within the ATP pocket, the rate limiting step of this enzyme [11]. Additionally, in the DFG-in confirmation Takinib can competitively inhibit ATP-binding of primarily activated TAK1, causing TNFα-induced apoptosis of the synovial fibroblasts involved in rheumatoid arthritis [12]. Takinib in general has shown therapeutic applications in inflammatory and autoimmune diseases as well as different types of cancer [11,12], however, the protective function of Takinib in TBI remains unknown. The objective of this study was to explore the possible anti-inflammatory and neuroprotective benefits gained from the use of Takinib in TBI rat models, and to determine how these actions could be regulated.

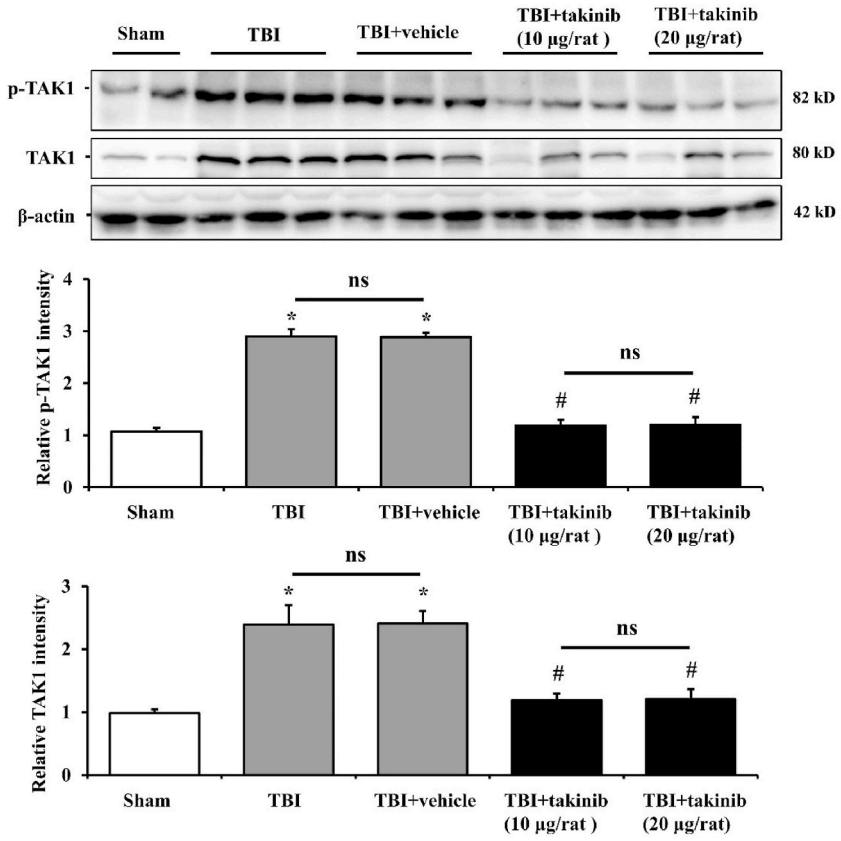

Fig. 1. Impact of Takinib administration on *p*-TAK1 and TAK1 levels at 24h post-TBI. *p*-TAK1 and TAK1 were significantly upregulated 24 h following a TBI. Takinib treatment suppressed *p*-TAK1 and TAK1 levels post-24 h following a TBI, contrary to the control group. No significant variations were observed among the two TBI groups. Quantitative findings utilized the format of mean ± standard deviation (n = 6); ns, no significance, $P > 0.05$; *, $P < 0.05$ versus the control group; #, $P < 0.05$ versus the TBI + vehicle group. Original images of Western blots are presented in Supplementary fig. 1.

2. Results

2.1. Takinib decreases the expression of TAK1 and p-TAK1 at the protein level in the cortex of rats at 24h post-TBI

The expression of TAK1 and *p*-TAK1 enzymes are typically increased dramatically by 24 h post-TBI [9]. To investigate the influence of Takinib on TAK1 activation, TBI-induction was performed using a modified of Feeney's weight-drop model, as previously described [9]. Day one post-procedure, the evaluation the two enzymes demonstrated upregulation in the injured cortex homogenates among TBI-operated rats, contrary to control rats which did not demonstrate this same increase. In contrary, administration of Takinib 30 min post-TBI was shown to downregulate the expression of TAK1 and *p*-TAK1 (Fig. 1, $P < 0.05$). Rats who received both 10 and 20 μg doses of Takinib observed similar decreases in TAK1 levels. No difference in efficacy was observed between the two doses. Overall, these findings demonstrated the effectiveness of Takinib in preventing an increase of TAK1 and *p*-TAK1 levels following a TBI.

2.2. Attenuation of TBI-induced neurological deficits following Takinib administration

For evaluation of the protective actions of Takinib among the rats, the neurological severity score (NSS) and beam walking scores were assessed 24 h post-TBI. Pre-treatment with Takinib, the NSS scores (Fig. 2A) were substantially higher, whereas the beam walking scores (Fig. 2B) were remarkably reduced in rats from the TBI group versus the control group. Both doses of Takinib (10 and 20 μg) noramlized the NSS and beam walking scores in rats post-TBI ($P < 0.05$). No variations of effectiveness were found between the two doses. Therefore, the lower dose of Takinib was employed in all subsequent studies. These findings highlight the potential neuroprotective effects of Takinib in TBI-affected rats.

2.3. Blocking IκB-α degradation and suppressing p65 nuclear translocation by Takinib, post-TBI

TAK1 plays an important role in the NF-κB pathway, leading to the evaluation of the impact Takinib has on NF-κB activation. Protein levels of IκB-α, an NF-κB activation indicator, appeared to decrease post-TBI. However, IκB-α degradation was shown to be inhibited following the administration of Takinib (Fig. 3A, $P < 0.05$). Furthermore, NF-κB activation has been shown to enhance the nuclear translocation of p65 subunits [13]. In this study, nuclear levels of p65 (Fig. 3B) were significantly higher, while its cytosolic levels (Fig. 3C) were lower post-TBI compared to the control procedure ($P < 0.05$). These changes were attenuated by Takinib administration (Fig. 3B, C, $P < 0.05$). Immunofluorescence analysis also revealed that the majority of the p65 protein was in the cytoplasm in the control group but was translocated to the nucleus in the post-TBI group. Takinib administration was demonstrated to inhibit the nuclear translocation of p65 (Fig. 3D, $P < 0.05$). It was concluded that TBI-induced activation of NF-κB was inhibited by Takinib via TAK1 inhibition.

2.4. Reduction in TBI-induced pro-inflammatory cytokines with Takinib administration

To explore the impact of Takinib on the TBI-induced inflammatory process, TNF-α and IL-1β levels in the injured cortex were assessed with the aid of ELISA. These levels were markedly elevated in post-TBI rats in contrast the control rats. A significant reduction

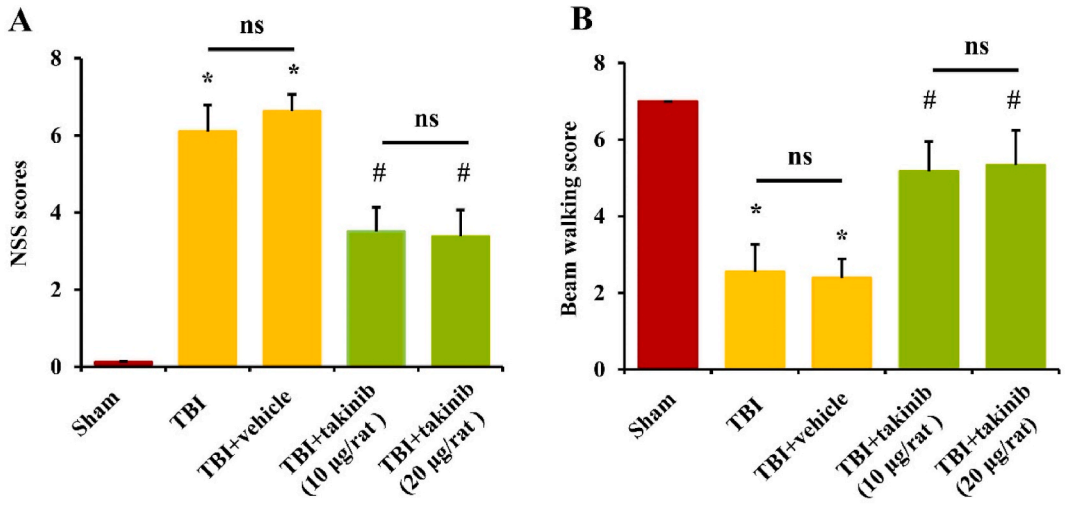

Fig. 2. Impact of Takinib on NSS and beam walking scores post-24 h in TBI-affected rats. The pre-treatment TBI group exhibited increased NSS scores (A) and reduced beam walking scores (B) as opposed to the control group. Takinib administration substantially enhanced the NSS score and increased beam walking. No significant variations were observed across the two TBI groups. Data are presented as mean ± standard deviation (n = 6); ns, no significance, $P > 0.05$; *, $P < 0.05$ versus the control group; #, $p < 0.05$ versus the TBI + vehicle group.

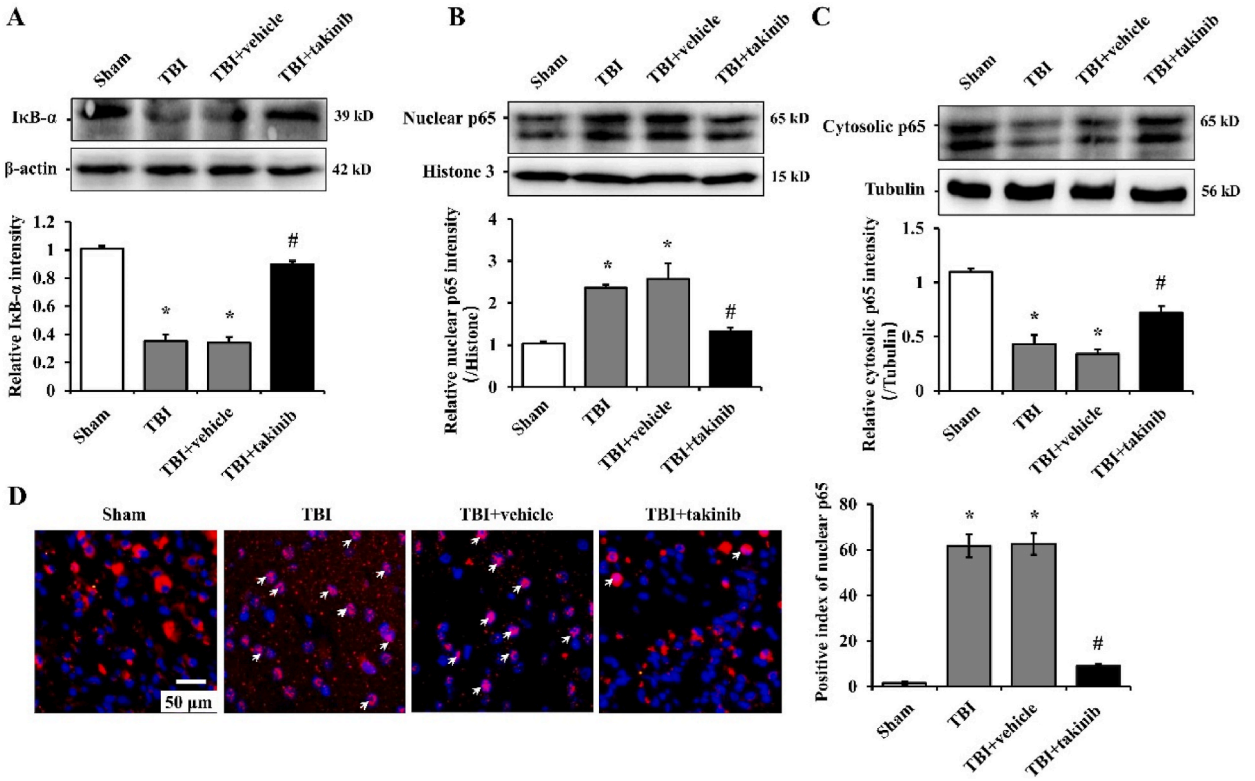

Fig. 3. Western blots of IκB-α and p65, and immunofluorescence representing nuclear translocation of p65 in cortex samples at 24h post-TBI. (A) IκB-α expression in rats post-TBI alone and TBI + vehicle was greatly reduced in comparison to the control rats. Takinib (10 μg) administration was shown to suppress TBI-induced downregulation of IκB-α. Nuclear p65 (B) was higher and cytosolic p65 (C) appeared reduced in the post-TBI and TBI + vehicle groups in contrast to the control group. Takinib (10 μg) administration reversed these effects, suppressing p65 nuclear translocation and enhancing cytosolic p65 levels. Normalization of the protein levels was observed on the β-actin, tubulin or histone 3 levels (n = 8). (D) Representative immunofluorescence images of p65. Nuclear translocation of p65 (red arrows) was significantly inhibited by Takinib (10 μg) administration post-TBI, as observed by the nuclei dyed blue with DAPI (n = 6). No remarkable variations were evident across the two TBI groups. Data are presented as mean ± standard deviation. *, $P < 0.05$ versus the control group; #, $P < 0.05$ versus the TBI + vehicle group. Original images of Western blots are presented in Supplementary fig. 2.

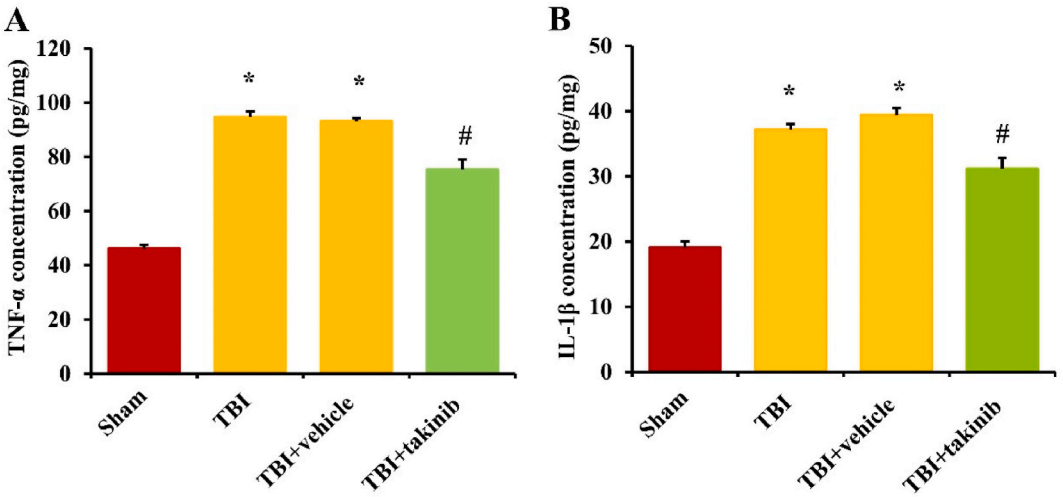

Fig. 4. Evaluation of post-TBI TNF-α and IL-1β protein levels by ELISA at 24h. TNF-α (A) and IL-1β (B) were upregulated post-TBI, and Takinib (10 μg) administration negated these effects. Outcomes are presented in terms of mean ± standard deviation (n = 8); *, $P < 0.05$ versus control; #, $P < 0.05$ versus TBI + vehicle.

in these levels was then observed following Takinib administration (Fig. 4A and B, $P < 0.05$), providing evidence that the inhibition of TAK1 can reverse the TBI-induced rise in cytokine levels.

2.5. Attenuation of TBI-induced BBB disruption and cerebral edema by Takinib administration

The impact of Takinib on blood-brain barrier (BBB) was scrutinized via detection methods for the presence of tight junction proteins zonula occludens-1 (ZO-1) and claudin-5. Western blot analysis depicted a reduction in these protein levels post-TBI in contrast to the control procedure. Takinib administration was observed to prevent this decrease (Fig. 5A, $P < 0.05$), indicating its effectiveness in reducing TBI-induced BBB disruption. Fig. 5B shows markedly increased cerebral water level in the rats post-TBI + vehicle compared to the control rats, which was followed by a significant reduction following Takinib administration (Fig. 5B, $P < 0.05$). These findings highlight the physiological protection against TBI effects obtained from drug, in addition to behavioral benefits.

2.6. Reduction of TBI-induced neural apoptosis by Takinib administration

The suppression of TAK1 prior to the deprivation of oxygen and glucose demonstrates protection for neurons against apoptosis both *in vitro* and *in vivo* settings [9,14]. To test the effects of Takinib on neuronal apoptosis *in vivo*, apoptosis-associated proteins levels were observed. Findings revealed a significant reduction in Bcl-2 levels and the Bcl-2/Bax ratio post-TBI as opposed to the control procedure, which was then negated following Takinib administration (Fig. 6A, $P < 0.05$). The levels of cleaved caspase 3, a well-established apoptosis indicator, were also evaluated using Western blotting (Fig. 6B). The findings depicted an upregulation in these levels in

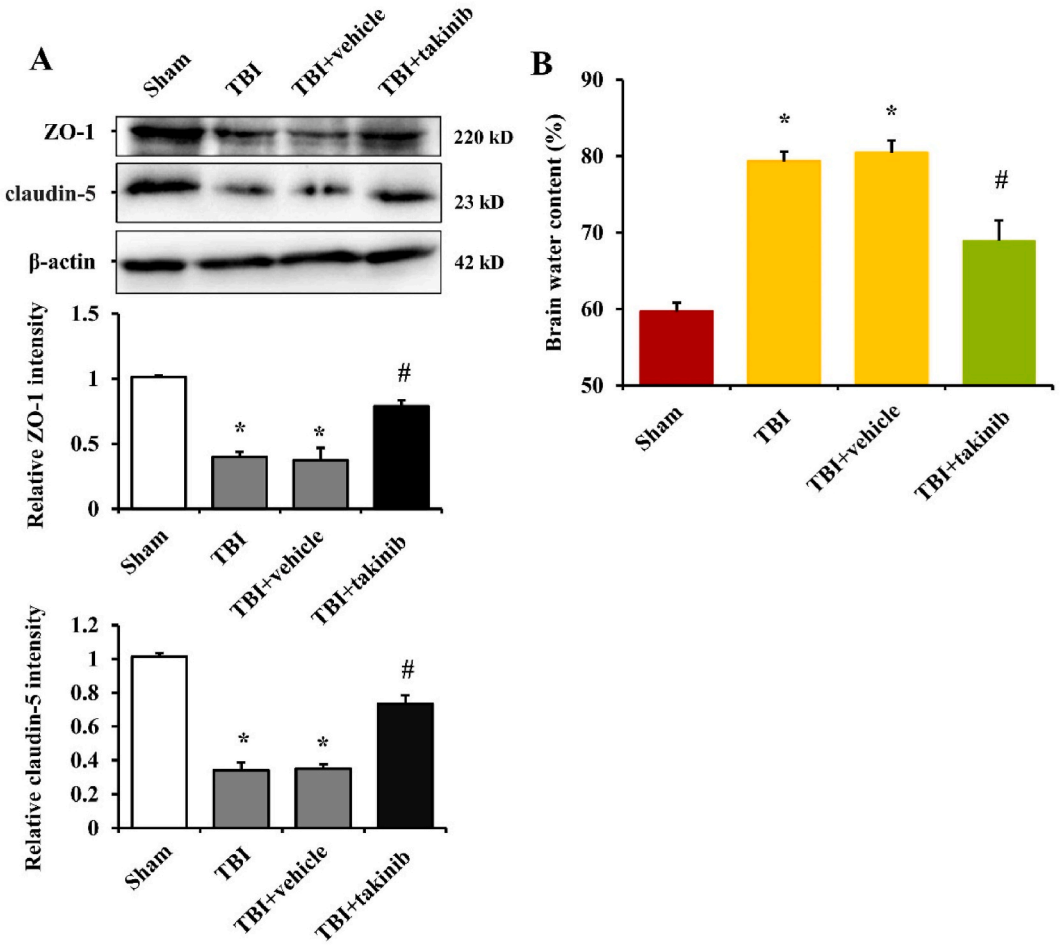

Fig. 5. The cortical impact of Takinib on cerebral edema and blood-brain barrier (BBB) at 24h post-TBI. (A) Images representing immunoblot bands and quantitative evaluation of ZO-1 and claudin-5 levels in the cortex post-TBI. Takinib (10 μg) administration shows reduction in TBI-induced BBB damage. (B) The cerebral water levels were obtained a day post-TBI. Takinib (10 μg) treated rats exhibited significantly reduced cerebral water levels as opposed to the TBI + vehicle group, whereas no remarkable variations were found across both TBI groups. Data are presented as mean ± standard deviation (n = 8); *, $P < 0.05$ versus the control group; #, $P < 0.05$ versus the TBI + vehicle group. Original images of Western blots are presented in Supplementary fig. 3.

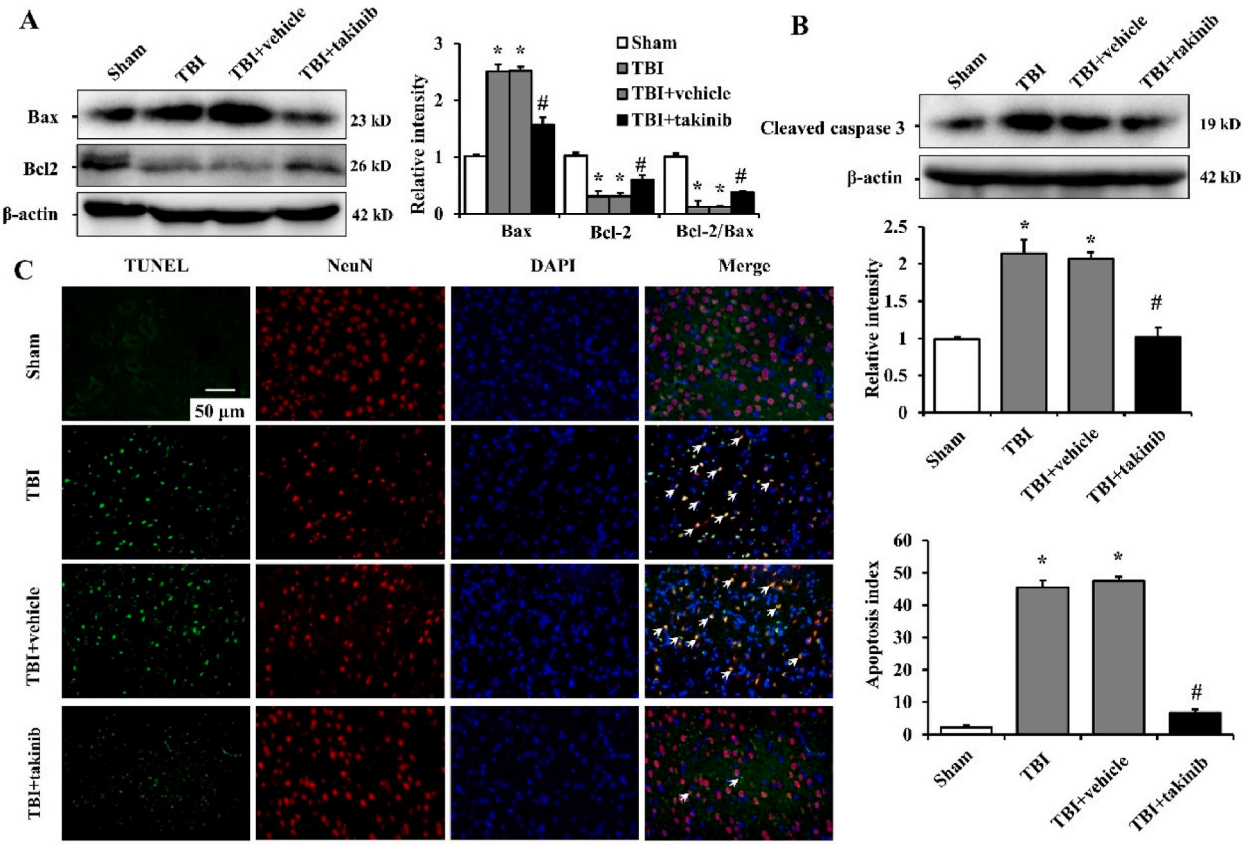

Fig. 6. Images representing Western blots of the Bcl2/Bax ratio and cleaved caspase 3 levels. The photomicrographs demonstrate NeuN (red) and TUNEL (green) double staining in cortex samples at 24h post-TBI. (A) Bax expression showed higher levels, while Bcl-2 levels were markedly reduced in both TBI groups as opposed to the control group. Takinib (10 μg) administration suppressed the TBI-induced variations in Bax and Bcl-2 levels. (B) Cleaved caspase 3 was upregulated in both TBI groups, contrary to the control group. Treatment with Takinib (10 μg) caused a decrease in levels of expression. Data are presented as mean ± standard deviation (n = 8). (C) Counterstaining of the nuclei was carried out with the aid of 4′,6-diamidino-2-phenylindole (blue). The TUNEL-positive cell counts increased post-TBI and decreased following Takinib (10 μg) administration. No remarkable variations were noted across both TBI groups. Data are presented as mean ± standard deviation (n = 6); *, $P < 0.05$ versus the control group; #, $P < 0.05$ versus the TBI + vehicle group. Original images of Western blots are presented in Supplementary fig. 4.

rats post-TBI + vehicle compared to the control procedure, which then showed a subsequent reduction in levels following administration of Takinib ($P < 0.05$).

Further evaluation of the apoptotic profiles among cortical neurons was performed using the terminal deoxynucleotidyl transferase dUTP nick end-labeling (TUNEL) assay. A small number of TUNEL-positive apoptotic cells appeared in the control rats in contrast to a larger number observed in the post-TBI rats (Fig. 6C). Takinib administration resulted in a significant reduction in apoptosis among neurons ($P < 0.05$). Collectively, these findings highlighted the capability of Takinib to mitigate TBI-induced neuronal apoptosis by exerting anti-apoptotic effects on the Bcl-2/Bax/cleaved caspase 3 signaling pathway.

2.7. Takinib administration conferred neuroprotection

The TBI-induced secondary brain injury led to morphological changes and inflammation-mediated reductions in neuronal viability. One day post-TBI, Nissl staining was conducted for morphological assessment and quantification of surviving cortical neurons. Morphologically (Fig. 7), the visual field of the post-TBI rats showed sparse cell arrangements, shrunken and dystrophic neurons, and loss of integrity in contrast to the intact and clear neurons among the control group. However, treatment with Takinib significantly improved the morphological appearance of the neurons ($P < 0.05$), demonstrating its neuroprotective effects after TBI.

3. Discussion

This study provides evidence for utilizing the TAK1 inhibitor Takinib as a treatment option for cases of TBI, helping to suppress the induced inflammation, apoptosis, and neuronal damage in rats. Consistent with these findings, Takinib administration was shown to cause significant downregulation of cleaved caspase 3, and pro-inflammatory cytokines TNF-α and IL-1β, with upregulation of ZO-1,

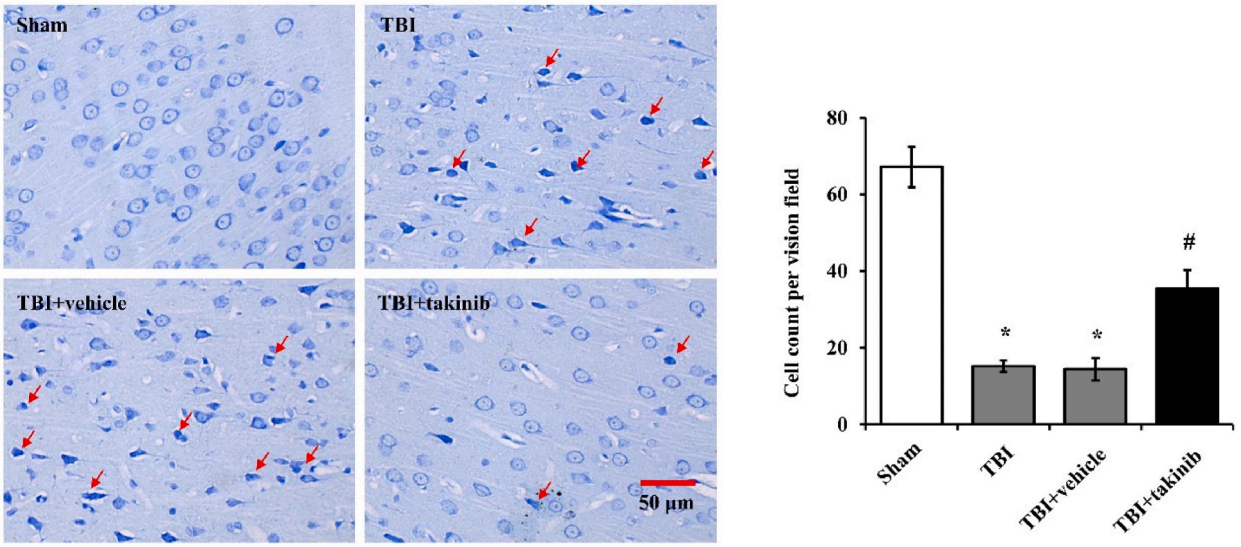

Fig. 7. Photomicrographs demonstrating Nissl staining in the rat cortex at 24h post-TBI. Vehicle-treated TBI-affected rats exhibited shrunken and dystrophic neurons. Takinib (10 μg) administration showed enhanced neuronal survival. The bar graphs illustrate the quantitative analysis. No remarkable variations were noted across both TBI groups. Data are presented as mean ± standard deviation (n = 6); *, $P < 0.05$ versus the control group; #, $P < 0.05$ versus the TBI + vehicle group.

claudin-5, and the Bax/Bcl-2 ratio. These neuroprotective effects were likely mediated by suppressing the TAK1/NF-κB/apoptosis signaling pathway.

TAK1 is a desirable target for anti-inflammatory therapy owing to its crucial role in the MAPK and NF-κB pathways. Previous studies by our group have demonstrated increased TAK1 activity post-TBI, resulting in exacerbation of SBI characterized by inflammation and neuronal apoptosis. Other studies have demonstrated that inhibition of TAK1 activity by (5Z)-7-oxozeaenol post-TBIalleviates inflammation and improves neurological recovery [9]. However, (5Z)-7-oxozeaenol also strongly inhibits a panel of at least 50 other kinases and forms covalent bonds with reactive cysteines during the activation process. This greatly limits its clinical translation due to potential off-target effects [15]. Takinib is a new TAK1 inhibitor and easily synthesized. In a kinome-wide screen, the molecule was found to exhibit extraordinary selectivity towards TAK1 over all other family members [11,16]. This rationale prompted the development of this study to further evaluate its neuroprotective role in patients with TBI and its potential as a treatment option.

Based preliminary evaluations and previous studies [11,17],drug concentrations of 10 and 20 μg administered with Intracerebroventricular (ICV) injections were selected as those doses have previously shown significant inhibition of TAK1 activity without toxicological adverse effects. After both doses demonstrated similar results, the lower of the two doses was later selected for all subsequent experiments in the study. An ICV injection of Takinib 30 min post-TBI inhibited the activity of TAK1 and ameliorated the manifestations of SBI, including inflammation, BBB damage, neurological impairments, and apoptosis in neurons. These outcomes support the neuroprotective effects of Takinib in TBI.

Emerging evidence strongly implicates inflammatory responses in overall TBI pathophysiology [18]. Pharmacological interventions that reduce cerebral inflammation could ameliorate SBI, highlighting a promising avenue for prevention of additional brain damage [19]. The kinase TAK1 is essential for IκB kinase-mediated activation of the NF-κB pathway [20]. Activation of the NF-κB/Rel transcription factors by nuclear translocation of specific cytoplasmic complexes plays a central role in inflammation through induction of proinflammatory gene transcription [21]. Our previous studies demonstrated that inhibition of TAK1 by 5Z-7-oxozeaenol significantly decreased NF-κB activity and subsequently the release of inflammatory cytokines [9]. Our current study results were consistent with previous findings, demonstrating that Takinib-mediated TAK1 inhibition led toreduced nuclear translocation of p65 in the cortex and the TBI-induced production of pro-inflammatory cytokines (TNF-α and IL-1β). Takinib had effectively inhibited the TAK1 activation and its downstream NF-κB inflammation signaling pathway.

One limitation of the study stems from how TBI can also lead to the activation of STAT3, and its inhibition can assist in reducing brain injury [22]. Interactions between Takinib and STAT3 were not explored in this study and the possibility of STAT3 inhibition contributing to the overall neuroprotective effects cannot be excluded. Future research should be conducted to explore the potential relationship between the two.

In addition to inflammation, cerebral edema and apoptosis in neurons represent two independent risk factors for mortality and unfavorable patient prognosis post-TBI [23,24]. Pro-inflammatory cytokines and chemokines produced via the activated inflammatory cells are critically involved in the disruption of the integrity of BBB. They achieve this by downregulating tight junction proteins and enhancing BBB permeability, resulting in cerebral edema [25]. In this study, the levels of two important tight junction proteins, ZO-1 and claudin-5, were assessed. These proteins were found to be decreased in TBI models versus the control. Treatment with Takinib substantially inhibited the degradation of ZO-1 and claudin-5, demonstrating protection of the BBB integrity and reducing cerebral

edema.

In a post-TBI brain, apoptosis is a significant mode of neuronal death that can result from both SBI and programmed cell death of senescent cells [26]. Treatment with Takinib was shown to significantly downregulate the expression of apoptosis-associated proteins, such as cleaved caspase-3 and Bax, and reduced the number of TUNEL-positive cells. Furthermore, Takinib administration reduced overall neuronal damage and improved their morphology, as observed using Nissl staining, which indicates enhanced neuronal survival post-TBI.

In summary, inhibition of TAK1 with Takinib assisted in preventing the release of inflammatory cytokines, reduced cerebral edema and neuronal apoptosis and enhanced the functioning of neurons in a TBI rat model. These findings highlight the neuroprotective impact of Takinib against TBI and its effects, suggesting that targeting TAK1-regulated signals can serve as a reliable method for pharmacological treatment. Takinib holds a high therapeutic potential for TBI-affected individuals.

4. Materials and methods

4.1. Animal ethics statement

The protocols for all animal experiments were in accordance with the local and international guidelines on the ethical use of laboratory animals. All procedures adopted in this study were approved by the Henan Polytechnic University Animal Care and Use Committee (Approval number: HPU2021-006), and conducted under the control of the national guidelines in China to minimize the number of laboratory animals used and the overall experienced.

4.2. Animal and TBI model

This study utilized male Sprague-Dawley rats weighing between 250 and 300 g. The animal subjects were kept in a controlled environment with alternating 12-h light/12-h dark cycles and unrestricted food and water supplies.

To induce TBI for experimental purposes, Feeney's weight-drop model was modified according to a method provided in previous research [9]. Anesthesia (phenobarbital sodium, 50 mg/kg) was administered to the subjects intraperitoneally while maintaining spontaneous breathing. A midline incision of 20 mm was made over the skull. The skin and fascia were then retracted, and a 5 mm diameter bone window was created over the right parietal region using a dental drill. The center of the bone window was created 1.5 mm behind and 2.5 mm laterally to the bregma. Throughout the process, the dura mater was kept intact. A steel weight of 40g with a flat end was released from a 25 cm height along a stainless-steel rod, hitting a small pillar (4 mm wide, 5 mm long) located on the dura mater. This process compressed the cortex to a depth of 5 mm.

Control animals underwent the same anesthesia and surgical procedure, however there was no contusion of the cortex. Core and cerebral temperatures were maintained between 36.8 and 37.2 °C with the aid of feedback warming lamps. The temperature was continuously monitored and tracked with rectal and temporalis muscle thermistors. Partial pressure of carbon dioxide (PaCO2) and pH of the arterial blood were analyzed intermittently to maintain normal physiological ranges. To maintain temperatures at approximately 37.0 °C, the rats were placed on a warming pad until they regained mobility. Post-consciousness, the rats were returned to their cages with an unrestricted food and water supplies.

4.3. Experimental groups and Takinib treatment

Two experiments were performed. In the first, Takinib purchased from Sigma (St. Louis, MO, USA) was dissolved in dimethylsulfoxide (DMSO) directly prior to administration. Takinib solutions (10 μg and 20 μg per 5 μL) or DMSO alone (5 μL) was administered via the ICV route 30 min after injury using a 10 μL Hamilton microsyringe [9]. Two concentrations of Takinib were used to evaluate its neuroprotective effects post-TBI. Under the effects of phenobarbital sodium anesthesia, each subject was securely placed in a stereotactic frame in preparation for the ICV injections.

Table 1
Neurological severity scoring.

Items	Description	Points	
		Success/failure	
Exit circle	Ability and initiative to exit a circle of 30 cm diameter (time limit: 3 min)	0	1
Mono-/hemiparesis	Paresis of upper and/or lower limb of contralateral side	0	1
Straight walk	Alertness, initiative, and motor ability to walk straight, when placed on the floor	0	1
Startle reflex	Innate reflex (flinching in response to a loud hand clap)	0	1
Seeking behavior	Physiological behavior as a sign of "interest" in the environment	0	1
Beam balancing	Ability to balance on a beam 7 mm in width for at least 10 s	0	1
Round stick balancing	Ability to balance on a round stick 5 mm in diameter for at least 10 s	0	1
Beam walk: 3 cm	Ability to cross a beam (length × width, 30 × 3 cm)	0	1
Beam walk: 2 cm	Same task but with increased difficulty (beam width = 2 cm)	0	1
Beam walk: 1 cm	Same task but with increased difficulty (beam width = 1 cm)	0	1
Maximum score			10

The injection was administered at a position 1.5 mm left, 1 mm below, and 4.4 mm deep with respect to the bregma [27], with an injection duration of 10 min. Takinib or vehicle (DMSO) treatment (n = 12 rats/group) was administered by an ICV injection 30 min post-TBI. Neurological deficits, along with beam walking scores, were assessed. One day post-TBI, the rats were deeply anesthetized, cerebral water levels were determined (n = 6), and brain tissue was collected (n = 6) to detect the levels of *p*-TAK1 and TAK1 expression.

In the second stage of the experiment, the rats were administered either Takinib (10 μg) or a vehicle half an hour post-TBI. After 24 h, all rats were anesthetized and transcardially perfused with 0.9 % saline. The brains of some of the rats were removed to be fixed in paraformaldehyde for histological sectioning. For the remaining rats, the surrounding brain tissue of the injured cortex (within 3 mm from the margin of the contusion site) was dissected on ice then immediately stored in liquid nitrogen [28]. These samples were later subjected to Western blot analysis and enzyme-linked immunosorbent assay (ELISA) (n = 8 rats/group).

4.4. Assessment of neurological behavior

The neurological condition of the rats was assessed at 24 h post-TBI with the aid of NSS. This scoring system evaluates the ability of the rats to accomplish ten separate tasks related to motor skills, alertness, and balance. The score ranges from 0 (minimum deficit) to 10 (maximum deficit), where each task not completed earns one point (Table 1) [29]. All of these tests were performed by two researchers who were blinded to the groups being assessed.

4.5. Beam walking score

The Takinib-treated rats and those receiving a vehicle were subjected to behavioral and functional tests 24 h post-TBI. These tests were implemented by an observer blinded to the conditions of the experiment. Each rat was trained to walk along a beam one day before the injury, and then again right before anesthesia was administered on the day of the injury.

The motor skills and coordination of animals were estimated by this score. The test was performed as previously described [28]. The beam walking potential was graded from 1 to 7, described below.

1. The rat couldn't place the damaged hind limb on the horizontal beam surface.
2. The rat placed the damaged limb on the beam and remained in balance but failed to walk across.
3. The rat dragged the damaged hind limb while walking the beam.
4. The rat walked the beam, placing the injured limb on the beam surface once.
5. The rat walked the beam, using the affected limb for support through less than half the steps.
6. The injured limb was used by the rat for more than half the steps.
7. A maximum of two-foot slips occurred while the rat walked across the beam. Seven was the highest possible score for non-operated rats.

4.6. Cerebral water content

As per techniques described in previous research, cerebral edema was assessed by employing the wet-dry method [10]. In brief, cerebral tissue around the contusion cortex was quickly collected and a wet weight measurement was carried out. These samples were then oven-dried at 110 °C for 24 h, Followed by a dry weight measurement. The total cerebral water content was derived from the following formula: percentage (%) of brain water = [(wet weight-dry weight)/wet weight] × 100.

4.7. Total/nuclear/cytosolic protein extraction

To obtain total protein from the cortex, tissues of appropriate size were mechanically lysed and added to a solution comprising 1 mM phenylmethylsulphonyl fluoride (PMSF), 20 mM Tris (pH 7.6), 0.2 % sodium dodecyl sulfate, 1 % Triton X-100, 0.11 IU/mL aprotinin, and 1 % deoxycholate (all sourced from Sigma, China). Following centrifugation at 14,000 rpm and 4 °C for 15 min, the resulting supernatant was gathered and preserved at −80 °C for further analytical procedures.

For the extraction of cortex nuclear proteins, a previously established protocol was utilized [10]. Homogenization of 50 mg of fresh cortex was carried out in a 0.4 mL ice-cold buffer A comprising of 2 mM $MgCl_2$, 0.1 mM ethylenediaminetetraacetic acid (EDTA), 10 mM KCl, 10 mM 4-(2-hydroxyethyl)-1-piperazineethanesulfonic acid (HEPES, pH 7.9), 1 mM dithiothreitol (DTT), and 0.5 mM PMSF (all supplied by Sigma, China). Fifteen microliters of Nonidet P-40 were introduced to this mixture.

Following centrifugation, the supernatant (cytoplasmic fraction) was collected, and the nuclear pellet was resuspended in 100 μL of buffer B, which comprised of 1 mM DTT, 20 mM HEPES (pH 7.9), 420 mM NaCl, 1.5 mM $MgCl_2$, 0.1 mM EDTA, 0.5 mM PMSF, and 25 % (v/v) glycerol. After centrifugation at 14,000 g and 4 °C for 15 min, the supernatant (nuclear fraction) was gathered and preserved at −80 °C for further analytical processes.

4.8. Western blot analysis

The surrounding brain tissue of the injured cortex was dissected on ice from less than 3 mm from the contusion site margin, then stored at −80 °C. The brain tissue segments were later homogenized on ice in 10 mM Tris-HCl buffer (pH 7.4), 10 mM EDTA,

containing 3 % Triton-100, 1 % SDS and 200 mM NaCl. The homogenized samples were then centrifuged at 13,000 g for 10 min at 4 °C. Following centrifugation, protein concentration in each sample was combined with BCA reagent (Sigma). Samples were then diluted (1:1) in a sample buffer (62.5 mM Tris-HCl, pH 6.8, 2 % SDS, 5 mM β-mercaptoethanol, 10 % glycerol), boiled for 5 min, and stored at −20 °C. To conduct Western blot analysis, each of the sodium dodecyl-sulfate polyacrylamide gel electrophoresis lanes were loaded with 40 μg of total or nuclear protein. The aforementioned proteins were subjected to the electrophoresis process and then transferred to a nitrocellulose membrane. The transfer protein-containing blot was blocked by a blocking buffer (1 × Tris-buffered saline comprising Tween 20 with 5 % w/v nonfat dry milk with no antibody) for an hour at 25 °C. The blot was then subjected to overnight incubation at 4 °C with primary TAK1 and *p*-TAK1 (Thr187) antibodies (1:200; Santa Cruz Biotech., CA), ZO-1, an inhibitor of NF-κB (IκB-α), cleaved caspase-3 (1:500; Cell Signaling Technology, MA), claudin-5, p65 (1:1,000, Abcam), β-actin, tubulin and histone 3 (1:1000; Proteintech, USA), Bcl-2 and Bax (1:500; Santa Cruz Biotech., CA). Following incubation with the secondary horseradish peroxidase-conjugated immunoglobulin G (IgG) the generated signal was detected with enhanced chemiluminescence detection reagents (Millipore Corporation, MA), which allowed for visualization of the blotted protein bands (Thermo Fisher Scientific). Using ImageJ software, relative alterations in protein levels were calculated via the mean pixel density and normalized to histone 3, tubulin or β-actin levels.

4.9. ELISA

Quantification of IL-1β and TNF-α levels in the cerebral tissue was achieved with the aid of ELISA kits for rats as per the specific protocols (Beyotime Biotechnology, China). The concentration of inflammatory cytokines in the cerebral tissue were presented as pg/mg protein.

4.10. TUNEL staining

The rats were perfused sequentially with saline and 4 % paraformaldehyde. The brains were extracted from the rats and kept in 4 % paraformaldehyde for one night. To eliminate water from the tissues, the brains were later immersed in 15 % sucrose for a day, then 30 % sucrose for an additional two days. Assessment of cerebral tissue apoptosis was achieved with the TUNEL assay (Roche, USA) as per the outlined protocol. The cerebral sections (15 μm thick) were exposed to TUNEL reaction buffer (50 μL), followed by a 1-h incubation period at 37 °C in a humid environment without light. This was followed by an overnight incubation period with an anti-NeuN antibody (1:200, Beyotime Biotechnology) at 4 °C. The sections were subjected to washing five times with phosphate-buffered saline (PBS) for 10 min each time and then incubation with secondary antibodies (Cy3-AffiniPure Goat Anti-Rabbit IgG (H + L), 1:200, Jackson, USA) for 2 h at 25 °C. Following this, the PBS washing process was repeated and the sections were stained for 5 min with the nuclear marker 4′,6-diamidino-2-phenylindole (DAPI, Beyotime Biotechnology). A Pannoramic MIDI digital slide scanner (3DHISTECH, Hungary) was used to generate images of the basal temporal lobe using fluorescence microscopy after three additional washes. The average number of TUNEL-positive cells in 10 microscopic fields (at 400× magnification) per section was then evaluated. A total of four sections from each animal were used for quantification. The final average of TUNEL-positive cells of the four sections was regarded as the total data for each sample. The graphs were created using the software CaseViewer (3DHISTECH, Hungary).

4.11. Nissl staining

The rats were administered anesthesia and transcardial perfusion was performed with saline and 4 % paraformaldehyde. Post-extraction, the brains of the rats were fixed in paraformaldehyde for 24 h. Following this fixation, the brains underwent dehydration and embedding in paraffin blocks. The brain samples were then sectioned into 4 μm slices and mounted on slides. Nissl staining was performed using Cresyl Violet, as per the previously described methods [30,31]. In the basal temporal lobe, the designated region for each subfield was marked, and cell counting was carried out on hte Cresyl Violet-stained neuronal cell bodies. Healthy neurons were observed to have large cell bodies, lightly stained cytoplasm, and spherical nuclei. Conversely, injured cells showed condensed nuclei, shrunken cell bodies, and darkly stained cytoplasm. Cell counting was performed using the same method from our previous study [9].

4.12. Immunofluorescence

The brain slices (4 μm-thick) were laid flat on adhesive glass slides. Initially, the slices were permeabilized with 0.3 % Triton X-100 for 30 min and blocked with goat serum for 1 h. They were then incubated at 4 °C overnight with the primary antibodies, rabbit anti-p65 (1:200, Abcam) followed by incubation with the secondary antibodies, Cy3 anti-rabbit IgG (Cy3-AffiniPure Goat Anti-Rabbit IgG (H + L), 1:200, Jackson, USA) for 2 h at 25 °C. Each step was followed by three times of a 5-min washing in PBS. The prepared specimens were counterstained with DAPI for 10 min and scanned with a Pannoramic MIDI digital slide scanner for image creations (3DHISTECH, Hungary). The localization of p65 expression was analyzed using Caseviewer software (3DHISTECH, Hungary).

4.13. Statistical analysis

The obtained findings were presented as means ± standard deviation (SD). A comparative analysis of the means across various study groups (except the neurobehavioral scores) was performed using a one-way analysis of variance method (ANOVA) followed by

Tukey's test. Contrarily, the neurobehavior scores of study subjects were assessed with the help of nonparametric tests (Kruskal–Wallis, and Dunn's post-hoc test). The SPSS v 16.0 (SPSS, Inc., IL) software was utilized to conduct statistical analysis of data. Variations in the data were deemed to be statistically significant at $P < 0.05$.

Ethical approval and consent to participate

All animal experiments were approved by Henan Polytechnic University Animal Care and Use Committee (Permit Number: HPU2021-006).

Data availability statement

The data presented in this study are available on request from the corresponding author.

CRediT authorship contribution statement

Shuangying Hao: Writing – original draft, Visualization, Validation, Project administration, Methodology, Funding acquisition, Formal analysis, Data curation. **Shuai Yuan:** Visualization, Methodology, Funding acquisition, Formal analysis, Data curation. **Zhiqiang Liu:** Visualization, Software, Methodology, Formal analysis, Data curation. **Baohua Hou:** Validation, Methodology. **Sijie Feng:** Validation, Supervision, Resources, Project administration. **Dingding Zhang:** Writing – original draft, Visualization, Validation, Methodology, Formal analysis, Data curation.

Declaration of competing interest

The authors declare that they have no known competing financial interests or personal relationships that could have appeared to influence the work reported in this paper.

Acknowledgements

This work was supported by the National Natural Science Foundation of China (NSFC, No. 32100951), the Science and Technology Project of Henan Province of China (No. 222102310267) and the Doctor Fund of Henan Polytechnic University (No. B2017–60, B2021-70).

Appendix A. Supplementary data

Supplementary data to this article can be found online at https://doi.org/10.1016/j.heliyon.2024.e29484.

References

[1] J.M. Garcia, A.B. Lopez-Rodriguez, Editorial: neuroendocrine disorders after traumatic brain injury: past, present and future, Front. Endocrinol. 10 (2019) 386.
[2] R. Diaz-Arrastia, P.M. Kochanek, P. Bergold, K. Kenney, C.E. Marx, C.J. Grimes, L.T. Loh, L.T. Adam, D. Oskvig, K.C. Curley, W. Salzer, Pharmacotherapy of traumatic brain injury: state of the science and the road forward: report of the Department of Defense Neurotrauma Pharmacology Workgroup, J. Neurotrauma 31 (2014) 135–158.
[3] T.K. McIntosh, K.E. Saatman, R. Raghupathi, D.I. Graham, D.H. Smith, V.M. Lee, J.Q. Trojanowski, The Dorothy Russell Memorial Lecture, The molecular and cellular sequelae of experimental traumatic brain injury: pathogenetic mechanisms, Neuropathol. Appl. Neurobiol. 24 (1998) 251–267.
[4] M.C. Morganti-Kossmann, L. Satgunaseelan, N. Bye, T. Kossmann, Modulation of immune response by head injury, Injury 38 (2007) 1392–1400.
[5] S.A. Robicsek, A. Bhattacharya, F. Rabai, K. Shukla, S. Dore, Blood-related toxicity after traumatic brain injury: potential targets for neuroprotection, Mol. Neurobiol. 57 (2020) 159–178.
[6] J. Ninomiya-Tsuji, K. Kishimoto, A. Hiyama, J. Inoue, Z. Cao, K. Matsumoto, The kinase TAK1 can activate the NIK-I kappaB as well as the MAP kinase cascade in the IL-1 signalling pathway, Nature 398 (1999) 252–256.
[7] S. Sato, H. Sanjo, K. Takeda, J. Ninomiya-Tsuji, M. Yamamoto, T. Kawai, K. Matsumoto, O. Takeuchi, S. Akira, Essential function for the kinase TAK1 in innate and adaptive immune responses, Nat. Immunol. 6 (2005) 1087–1095.
[8] J.H. Shim, C. Xiao, A.E. Paschal, S.T. Bailey, P. Rao, M.S. Hayden, K.Y. Lee, C. Bussey, M. Steckel, N. Tanaka, G. Yamada, S. Akira, K. Matsumoto, S. Ghosh, TAK1, but not TAB1 or TAB2, plays an essential role in multiple signaling pathways in vivo, Genes Dev. 19 (2005) 2668–2681.
[9] D. Zhang, Y. Hu, Q. Sun, J. Zhao, Z. Cong, H. Liu, M. Zhou, K. Li, C. Hang, Inhibition of transforming growth factor beta-activated kinase 1 confers neuroprotection after traumatic brain injury in rats, Neuroscience 238 (2013) 209–217.
[10] H.S. Zhang, H. Li, D.D. Zhang, H.Y. Yan, Z.H. Zhang, C.H. Zhou, Z.N. Ye, Q. Chen, T.W. Jiang, J.P. Liu, C.H. Hang, Inhibition of myeloid differentiation factor 88 (MyD88) by ST2825 provides neuroprotection after experimental traumatic brain injury in mice, Brain Res. 1643 (2016) 130–139.
[11] J. Totzke, D. Gurbani, R. Raphemot, P.F. Hughes, K. Bodoor, D.A. Carlson, D.R. Loiselle, A.K. Bera, L.S. Eibschutz, M.M. Perkins, A.L. Eubanks, P.L. Campbell, D. A. Fox, K.D. Westover, T.A.J. Haystead, E.R. Derbyshire, Takinib, a selective TAK1 inhibitor, broadens the therapeutic efficacy of TNF-alpha inhibition for cancer and autoimmune disease, Cell Chem. Biol. 24 (2017) 1029–1039 e1027.
[12] P.M. Panipinto, A.K. Singh, F.S. Shaikh, R.J. Siegel, M. Chourasia, S. Ahmed, Takinib inhibits inflammation in human rheumatoid arthritis synovial fibroblasts by targeting the janus kinase-signal transducer and activator of transcription 3 (JAK/STAT3) pathway, Int. J. Mol. Sci. 22 (2021).
[13] Y.C. Hu, Q. Sun, W. Li, D.D. Zhang, B. Ma, S. Li, W.D. Li, M.L. Zhou, C.H. Hang, Biphasic activation of nuclear factor kappa B and expression of p65 and c-Rel after traumatic brain injury in rats, Inflamm. Res. 63 (2014) 109–115.

[14] M. Neubert, D.A. Ridder, P. Bargiotas, S. Akira, M. Schwaninger, Acute inhibition of TAK1 protects against neuronal death in cerebral ischemia, Cell Death Differ. 18 (2011) 1521–1530.
[15] J. Wu, F. Powell, N.A. Larsen, Z. Lai, K.F. Byth, J. Read, R.F. Gu, M. Roth, D. Toader, J.C. Saeh, H. Chen, Mechanism and in vitro pharmacology of TAK1 inhibition by (5Z)-7-Oxozeaenol, ACS Chem. Biol. 8 (2013) 643–650.
[16] S.A. Scarneo, P.F. Hughes, K.W. Yang, D.A. Carlson, D. Gurbani, K.D. Westover, T.A.J. Haystead, A highly selective inhibitor of interleukin-1 receptor-associated kinases 1/4 (IRAK-1/4) delineates the distinct signaling roles of IRAK-1/4 and the TAK1 kinase, J. Biol. Chem. 295 (2020) 1565–1574.
[17] S.A. Scarneo, L.S. Eibschutz, P.J. Bendele, K.W. Yang, J. Totzke, P. Hughes, D.A. Fox, T.A.J. Haystead, Pharmacological inhibition of TAK1, with the selective inhibitor takinib, alleviates clinical manifestation of arthritis in CIA mice, Arthritis Res. Ther. 21 (2019) 292.
[18] K.N. Corps, T.L. Roth, D.B. McGavern, Inflammation and neuroprotection in traumatic brain injury, JAMA Neurol. 72 (2015) 355–362.
[19] T.T. Postolache, A. Wadhawan, A. Can, C.A. Lowry, M. Woodbury, H. Makkar, A.J. Hoisington, A.J. Scott, E. Potocki, M.E. Benros, J.W. Stiller, Inflammation in traumatic brain injury, J Alzheimers Dis 74 (2020) 1–28.
[20] G. Takaesu, R.M. Surabhi, K.J. Park, J. Ninomiya-Tsuji, K. Matsumoto, R.B. Gaynor, TAK1 is critical for IkappaB kinase-mediated activation of the NF-kappaB pathway, J. Mol. Biol. 326 (2003) 105–115.
[21] A.B. Kunnumakkara, B. Shabnam, S. Girisa, C. Harsha, K. Banik, T.B. Devi, R. Choudhury, H. Sahu, D. Parama, B.L. Sailo, K.K. Thakur, S.C. Gupta, B. B. Aggarwal, Inflammation, NF-kappaB, and chronic diseases: how are they linked? Crit. Rev. Immunol. 40 (2020) 1–39.
[22] B. Liu, G. Zhang, S. Cui, G. Du, Inhibition of RNF6 alleviates traumatic brain injury by suppressing STAT3 signaling in rats, Brain Behav 10 (2020) e01847.
[23] K. Ding, J. Xu, H. Wang, L. Zhang, Y. Wu, T. Li, Melatonin protects the brain from apoptosis by enhancement of autophagy after traumatic brain injury in mice, Neurochem. Int. 91 (2015) 46–54.
[24] Z. Wang, Z. Wang, A. Wang, J. Li, J. Wang, J. Yuan, X. Wei, F. Xing, W. Zhang, N. Xing, The neuroprotective mechanism of sevoflurane in rats with traumatic brain injury via FGF2, J. Neuroinflammation 19 (2022) 51.
[25] E.A. Winkler, D. Minter, J.K. Yue, G.T. Manley, Cerebral edema in traumatic brain injury: pathophysiology and prospective therapeutic targets, Neurosurg. Clin. 27 (2016) 473–488.
[26] W. Zhang, J. Hong, H. Zhang, W. Zheng, Y. Yang, Astrocyte-derived exosomes protect hippocampal neurons after traumatic brain injury by suppressing mitochondrial oxidative stress and apoptosis, Aging (Albany NY) 13 (2021) 21642–21658.
[27] S.M. Krieg, S. Sonanini, N. Plesnila, R. Trabold, Effect of small molecule vasopressin V1a and V2 receptor antagonists on brain edema formation and secondary brain damage following traumatic brain injury in mice, J. Neurotrauma 32 (2015) 221–227.
[28] X. Su, H. Wang, J. Zhao, H. Pan, L. Mao, Beneficial effects of ethyl pyruvate through inhibiting high-mobility group box 1 expression and TLR4/NF-kappaB pathway after traumatic brain injury in the rat, Mediat. Inflamm. 2011 (2011) 807142.
[29] M.A. Flierl, P.F. Stahel, K.M. Beauchamp, S.J. Morgan, W.R. Smith, E. Shohami, Mouse closed head injury model induced by a weight-drop device, Nat. Protoc. 4 (2009) 1328–1337.
[30] H. Yan, D. Zhang, S. Hao, K. Li, C.H. Hang, Role of mitochondrial calcium uniporter in early brain injury after experimental subarachnoid hemorrhage, Mol. Neurobiol. 52 (2015) 1637–1647.
[31] D. Zhang, H. Zhang, S. Hao, H. Yan, Z. Zhang, Y. Hu, Z. Zhuang, W. Li, M. Zhou, K. Li, C. Hang, Akt specific activator SC79 protects against early brain injury following subarachnoid hemorrhage, ACS Chem. Neurosci. 7 (2016) 710–718.